On the determination of Jupiter's satellite-dependent Love numbers from Juno gravity data

Virginia Notaro[a,*], Daniele Durante[a], Luciano Iess[a]

[a] Department of Aerospace and Mechanical Engineering,

Sapienza University of Rome, Rome, Italy

*** Corresponding author:** Virginia Notaro

Institution: Sapienza University of Rome

Address: Via Eudossiana 18, 00184, Rome, Italy

Email: virginia.notaro@uniroma1.it

Phone: +390644585976

Accepted manuscript, Planetary and Space Science (https://doi.org/10.1016/j.pss.2019.06.001)

Abstract

The Juno gravity experiment, among the nine instruments onboard the spacecraft, is aimed at studying the interior structure of Jupiter to gain insight into its formation. Doppler data collected during the first two gravity-dedicated orbits completed by Juno around the gas giant have already provided a measurement of Jupiter's gravity field with outstanding accuracy, answering crucial questions about its interior composition. The large dataset that will be collected throughout the remaining phases of the mission until the end in July 2021 might allow to determine Jupiter's response to the satellite-dependent tidal perturbation raised by its moons, and even to separate the static and dynamic effects.

We report on numerical simulations performed over the full science mission to assess the sensitivity of Juno gravity measurements to satellite-dependent tides on Jupiter. We assumed a realistic simulation scenario that is coherent with the result of data analysis from the first gravity passes. Furthermore, we implemented a satellite-dependent tidal model within the dynamical model used to fit the simulated Doppler data.

The formal uncertainties resulting from the covariance analysis show that Juno is indeed sensitive to satellite-dependent tides on Jupiter raised by the inner Galilean satellites (the static Love numbers of degree and order 2 of Io, Europa and Ganymede can be determined respectively to 0.28%, 4.6% and 5.3% at 1 sigma). This unprecedented determination, that will be carried out towards the end of the mission, could further constrain the interior structure of the planet, allowing to discern among interior models and improving existing theories of planetary tidal response.

Keywords: Jupiter; Tides; Radio science; Orbit Determination

1. Introduction

On July 4, 2016, the Juno spacecraft reached Jupiter and since then it has been orbiting the planet, studying its internal composition, magnetosphere and atmosphere to gain insight into the formation of the solar system itself (Bolton et al, 2017). Among the suite of nine instruments onboard the spacecraft, the gravity science investigation is aimed at measuring Jupiter's gravity field to characterize its interior mass distribution, the presence and structure of a core, and the rotational state of the planet. The Jovian gravity field is determined by accurately measuring the Doppler shift experienced by microwave signals sent to the spacecraft by an Earth station and then transponded back, preserving phase coherence, to the same station (two-way Doppler tracking configuration) (Asmar et al, 2017). The Doppler measurements are then processed with an orbit determination code, which includes a least-square filter and an accurate dynamical model of the spacecraft. As a result,

35 Juno's trajectory is reconstructed and several parameters are estimated, including the spherical
36 harmonic coefficients of Jupiter's gravity field.
37 After six orbits, two of which dedicated to the gravity experiment, Juno has provided crucial clues
38 about the interior of Jupiter, suggesting the existence of a diffused core where heavy elements are
39 diluted up to half the radius of the planet (Wahl et al, 2017). The unprecedented measurement of
40 Jupiter's North-South asymmetric gravity field has allowed to constrain the depth of Jupiter's zonal
41 winds to a few thousands of kilometers (Guillot et al, 2018; Iess et al, 2018; Kaspi et al, 2018). With
42 many orbits still left to complete (the nominal mission includes 35 revolutions around Jupiter, out of
43 which 25 are gravity-dedicated), Juno will continue to investigate fine features of Jupiter's gravity
44 field that can only be accessed with the end-of-mission set of measurements. In particular, the
45 determination of Jupiter's polar moment of inertia through the analysis of the motion of its spin-axis
46 is a key future objective of the Juno gravity experiment and will be relevant for discerning among
47 models of the gas giant's interior structure (Le Maistre et al, 2016).
48 As the mission progresses, the Juno gravity experiment will become more sensitive to the
49 gravitational signature of tides raised on Jupiter by its moons. An unconstrained measurement of
50 Jupiter's tidal response will only be possible with the uniform longitudinal sampling available at the
51 end of Juno's nominal mission. In particular, the total tidal perturbation exerted on Jupiter by its
52 satellites can be thought as the superposition of individual terms that depend on the mean motion of
53 each satellite. With a sufficiently large dataset and a favorable observation geometry, it could be
54 possible to separate the total tidal response of Jupiter into the single terms due to each satellite; in this
55 paper, we refer to this as *satellite-dependent* tidal response. This effect has first been studied with
56 numerical simulations, that show that Jupiter's fast rotation (and thus its large oblateness) introduces
57 a variation of its static tidal response with the distance between the gas giant and the perturber (Wahl
58 et al, 2016). In addition, resonances between the tidal forcing frequency (that depends on the satellite
59 orbital frequency) and Jupiter's natural oscillations eigenfrequencies, which determine the gas giant's
60 dynamical tidal response, might introduce further dependency of the tidal response on the perturbing

61 body. Note that, since each Galilean satellite induces a perturbation at a particular discrete frequency,
62 Jupiter's dynamical satellite-dependent tidal response is indeed *frequency-dependent*.
63 Satellite-dependent (or frequency-dependent if dynamical effects are considered) tides are not
64 currently included in the dynamical model used for the gravity investigation (Iess et al, 2018), nor a
65 complete dynamical tidal theory has been developed to predict the entity of this effect on gas giant
66 planets. The absence of theoretical modeling is partly due to the fact that previous gravity science
67 investigations of gas giants, such as that of the Cassini mission to Saturn, were essentially insensitive
68 to the satellite-dependent dynamical tidal response of the central planet, either because of unfavorable
69 orbital geometry or insufficient data. The determination of frequency-dependent tides on Jupiter with
70 Juno gravity data would be unprecedented and would provide further insight into the interior
71 composition and seismology of the gas giant (Guillot et al, 2004).
72 We present the results of numerical simulations aimed at evaluating the sensitivity of the Juno
73 gravity experiment to satellite-dependent tides on Jupiter, considering Doppler measurements over
74 the full extent of the scientific mission. To this aim, we modified the tidal model used within the orbit
75 determination process, and then performed a covariance analysis assuming realistic measurement
76 noise. The structure of this work is as follows: in Section 2 we briefly describe the theoretical
77 background with application to the Jupiter system, followed by a description of the numerical
78 simulation setup (Section 3). Section 4 discusses the results of the analysis, while the main
79 conclusions are outlined in Section 5.
80
81 **2. Tides on Jupiter**
82
83 Tides are raised on a central planet as the gravitational attraction from a perturbing body changes
84 across the planet. The deformation induced on the central body by the tidal perturbation (and the
85 consequent change of its gravitational potential) can be measured with Doppler radio tracking data

from an orbiter or flyby spacecraft. The following provides a brief overview of tidal theory applied to the Jupiter system.

The external gravity field of Jupiter is described by the spherical harmonic expansion of the gravitational potential (Kaula, 1966):

$$V(r,\theta,\lambda) = \frac{\mu}{r}\left(1 + \sum_{l=2}^{\infty}\sum_{m=0}^{l}\left(\frac{R}{r}\right)^{l}\left(\bar{C}_{lm}\cos m\lambda + \bar{S}_{lm}\sin m\lambda\right)\bar{P}_{lm}(\cos\theta)\right) \quad (1)$$

where R and μ are respectively the reference radius of Jupiter (R = 71492 km) and its gravitational parameter (μ = 126686534.19 km^3/s^2), and (r,θ,λ) are the spherical coordinates. $\bar{C}_{lm}$, $\bar{S}_{lm}$ are the fully normalized coefficients of degree l and order m, while $\bar{P}_{lm}$ is the normalized associated Legendre polynomial. The gravitational potential of the gas giant, perturbed by the tide, is proportional to the perturbing potential through the Love numbers k_{lm} (Love, 1911). Consequently, the effect of tides on the gravity field of Jupiter can be related to a change of the gravity field spherical harmonic coefficients (Gavrilov et al, 1976; Moyer, 2003; Murray and Dermott, 1996)

$$\Delta\bar{J}_l = -\frac{1}{2l+1}\,k_{l0}\sum_j \frac{\mu_j}{\mu}\left(\frac{R}{r_j}\right)^{l+1}\bar{P}_{l0}(u_j), \quad (2)$$

$$\Delta\bar{C}_{lm} - i\Delta\bar{S}_{lm} = \frac{1}{2l+1}k_{lm}\sum_j \frac{\mu_j}{\mu}\left(\frac{R}{r_j}\right)^{l+1}\bar{P}_{lm}(u_j)(s_j - it_j)^m.$$

In Equation (2), μ, μ_j are the gravitational parameters of Jupiter and the j-th satellite, respectively, whilst r_j is the radial distance from the planet to the j-th satellite. Finally, s_j, t_j, u_j are the three Cartesian components of the unit body-fixed vector from Jupiter to the j-th perturbing body.

The tidal response of Jupiter and Saturn due to their numerous moons has been extensively studied with numerical simulations and a wide range of astrometric observations (Guillot et al, 2004; Lainey

et al, 2017). The rapid rotation of the two gas giants, and thus the large oblateness, intensifies the tidal response and introduces a splitting of the Love numbers of the same degree and different order, which for terrestrial planets are commonly considered equal as past deep-space planetary exploration missions to Mars, Venus or Mercury have not provided the data coverage or accuracy necessary to disentangle those parameters. Concerning the Jupiter system, only the k_{lm} with even $l-m$ are computed in the numerical models, as the out-of-plane tidal perturbation corresponding to odd $l-m$ is negligible due to the near-equatorial orbits of the satellites (Wahl et al, 2017).

The large oblateness of Jupiter leads to a variation of its static (i.e., equilibrium) tidal response with the perturbing body. Wahl et al, 2016 published the first prediction of Jupiter's satellite-dependent static Love numbers. In particular, the k_{22} resulting from their model is equal to 0.58999, 0.58964 and 0.58949 respectively for Io, Europa and Ganymede (see Table 4 in Wahl et al, 2016), showing small but non-negligible discrepancies with Jupiter models that consider only the tidal response to the satellite Io (the major contributor).

Wahl et al, 2016 assumed a simplified tidal model that does not account for the relative motion between the satellites and Jupiter, thus leaving out any dynamical effect from their analysis. In fact, the frequency of the tidal perturbation associated with the motion of each satellite could excite Jupiter's natural oscillation modes, amplifying its satellite-dependent tidal response and thus the differences among the Love numbers pertaining to the different satellites. In this regard, Vorontsov et al, 1984 developed a dynamical tidal theory for a non-rotating Jupiter by solving the small adiabatic oscillation equations including the tidal potential generated by a moon in a circular orbit around the planet. The maximum difference between their satellite-dependent Love numbers, that depend on Jupiter's natural oscillation eigenfrequencies, and the ones from the static non-rotating model in Gavrilov and Zharkov, 1977 is about 1.2% on k_2, suggesting that dynamical effects are not relevant. However, this theory is incomplete as it does not account for the rotational enhancement of Jupiter's tidal response (Wahl et al, 2017).

A complete dynamical theory of Jupiter's response to tides produced by the Galilean satellites orbiting around the planet with different periods has not been developed yet. Nevertheless, a first-order evaluation on the entity of this effect can be obtained firstly with the tidal parameter q_T, which describes the magnitude of the tidal perturbation produced by each satellite on Jupiter (Wahl et al, 2017)

$$q_T = -3\frac{\mu_j}{\mu}\left(\frac{R}{a_j}\right)^3, \quad (3)$$

where a_j is the semi-major axis of the satellite. Since the change in the harmonic coefficients due to tides depends on the tidal parameter (Equation (2)), q_T can be used as a measure of the strength of the tidal forcing. Table 1 lists the tidal parameter, the orbital period, as well as the frequency of the tidal perturbation relative to Jupiter ($\Omega_j - \omega_{JUP}$), for the Galilean satellites, Amalthea, Adrastea, Metis, Thebe and the Sun. In the table, ω_{JUP} and Ω_j are respectively Jupiter's rotation rate and the mean motion of the j-th perturber. Although dominated by the fast rotation of the planet, the quantity $\Omega_j - \omega_{JUP}$ shows a dependency on the perturbing body. The accurate gravity measurements collected from the Juno spacecraft might allow to determine and separate the different contributions.

Table 1: Tidal parameter, orbital period, and tidal forcing frequency relative to Jupiter for Io, Europa, Ganymede and Callisto, as well as the Amalthea satellite system and the Sun. The bodies are ordered according to the tidal parameter.

Body	**$-q_T$ (x10^8)**	**Orbital Period (h)**	**$\Omega_j - \omega_{JUP}$ (x10^{-4}rad/s)**
Io	68.6	42.46	-1.35
Europa	9.2	85.2	-1.55

Ganymede	6.9	171.7	-1.66
Callisto	0.9	400.56	-1.71
Sun	0.24	11.9 years	-1.76
Amalthea	0.021	11.76	-0.31
Thebe	0.0079	16.18	-0.67
Metis	0.0032	7.08	-0.73
Adrastea	0.0002	7.15	-0.73

3. The Juno gravity experiment

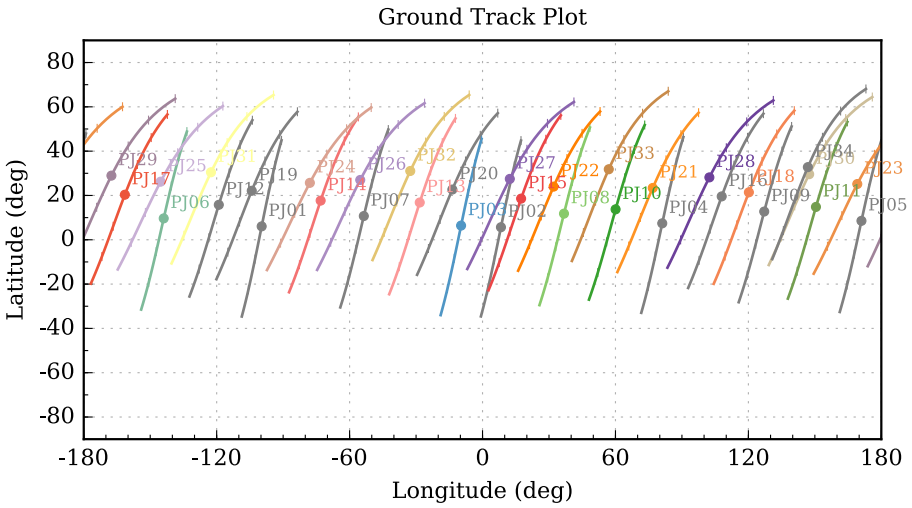

Figure 1: Juno's nominal mission ground tracks over Jupiter. Longitudes are expressed in Jupiter's System III reference frame. Tracks are plotted for a 30-minute window around the pericenter, which is indicated by a full dot. Tick spacing is 5 minutes. Nominally, the Juno spacecraft altitude ranges from 11000-12500 km over the 1-bar cloud tops at the beginning of the tracks to about 3000-8000 km at the pericenter. Gray tracks belong to passages not dedicated to the gravity science experiment, and thus not included in this analysis.

166 During its 52.9-day orbit around Jupiter, Juno uses its suite of nine instruments to study Jupiter's
167 magnetic, gravity fields and its atmospheric dynamics. In particular, the gravity experiment involves
168 the measurement of the Doppler shift of microwave signals transmitted from NASA's Deep Space
169 Station (DSS) 25 (from the Deep Space Network Communication Complex in Goldstone, California)
170 to the spacecraft and then transponded, preserving phase coherence, back to the same station. Gravity
171 measurements are carried out as the spacecraft approaches the pericenter of its orbit since the Doppler
172 signal provides the most sensitivity to Jupiter's gravity field. This requires the spacecraft High Gain
173 Antenna (HGA) to be pointed towards the Earth. For MicroWave Radiometer (MWR) observations,
174 instead, the MWR antennas (located on the side of Juno's main bus) must be nadir-pointed,
175 preventing coherent link to ground trough the HGA. As a result, out of the 35 orbits around Jupiter
176 planned until the end of the science mission, only 25 are dedicated to the gravity experiment. Figure
177 1 shows Juno's ground tracks from orbital insertion to end-of-mission in July 2021. The colored
178 tracks belong to the gravity-dedicated passages. The longitude of the closest approach, typically about
179 4000 km over the 1-bar cloud tops, drifts as the orbit changes during the mission so as to obtain a
180 complete map of Jupiter at end-of-mission.

181 The nominal tracking configuration during gravity-dedicated passages consists of a 6-hour two-
182 way link from the DSS 25 antenna at X- and Ka-band (7.2 and 32 GHz) simultaneously. The link is
183 established as long as the elevation angle of the antenna is larger than 15 degrees. Furthermore, two-
184 way tracking from DSS 43 at X-band is routinely acquired after the pericenter for navigation
185 purposes. This additional dataset is used for the gravity field analysis as well, prior to an Orbit Trim
186 Maneuver performed a few hours after the pericenter. Thanks to the onboard and ground
187 instrumentation, the measurements are accurate down to 0.01 mm/s at 60-s integration time (Asmar
188 et al, 2017). After tracking, the Doppler data are processed using a least-square estimation filter that
189 minimizes the difference between the observed measurements and the ones computed using a
190 complete dynamical model of the spacecraft's trajectory. The filter provides an estimate of the
191 spacecraft state, along with a set of solve-for parameters (see Section 3.4).

192

193 *3.1 Determining satellite-dependent tides with Juno gravity data*

194 The geometry of Juno's orbit and of the Jovian moons is crucial for the determination of Jupiter's
195 satellite-dependent tides. To sample Jupiter's tidal bulge due to one satellite, the longitudes of that
196 satellite over each gravity-dedicated pericenter passage should be uniformly-distributed. The
197 longitudinal separation among the moons should also vary throughout the 25 gravity orbits to allow
198 separating Jupiter's satellite-dependent tidal response.

199 Figure 2 shows that Juno's trajectory assures adequate longitudinal coverage for tides raised by
200 Io, Europa and Ganymede, but not by Callisto (essentially due to the insufficient time span of the
201 mission). However, Juno's 52.9-day orbital period is close to resonance with Io, which is locked in a
202 4:2:1 Laplace resonance with Europa and Ganymede. Thus, the longitudinal separation of Io and
203 Europa (the satellites with the largest tidal parameters) is almost null for the first gravity orbits (full
204 circles in Figure 3), while slowly drifting to about 45 degrees at the end-of-mission. Consequently, a
205 reliable separation of the satellite-dependent tidal perturbations will require data collected over the
206 full mission.

207

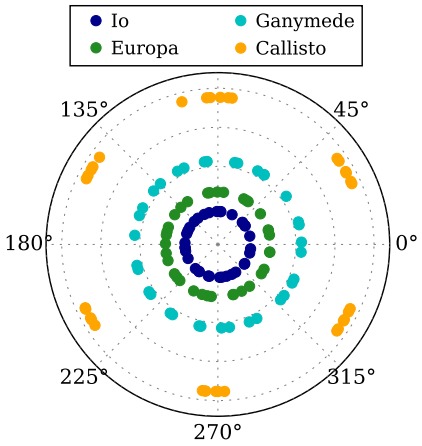

208

209 **Figure 2:** Difference between the longitude of Io (blue dots),
210 Europa (green dots), Ganymede (cyan dots) and Callisto (yellow
211 dots) and Juno's longitude for each of the gravity-dedicated
212 pericenter passes. Juno's longitude is fixed at 0 degrees.

213

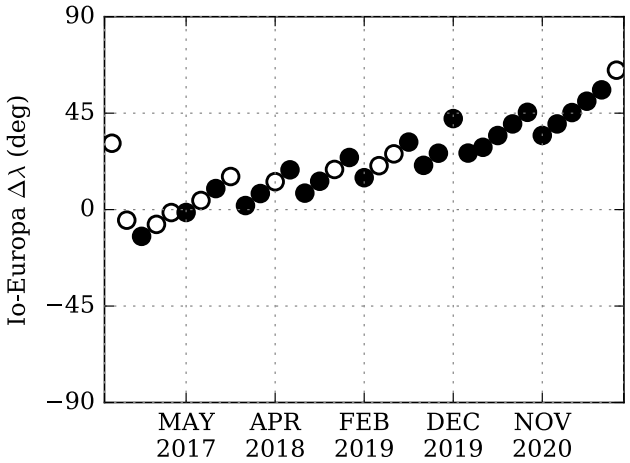

214

215 **Figure 3:** Difference between Io and Europa longitudes for each of the Juno pericenter
216 passages until end-of-mission. Full circles refer to passes dedicated to gravity.

217

218 *3.2 Simulation description*

We ran numerical simulations of Juno's gravity experiment using the JPL/NASA MONTE (Mission analysis, Operations and Navigation Toolkit Environment) navigation and orbit determination software (Smith et al, 2016). We simulated Juno Doppler measurements assuming the nominal tracking configuration for each of the 25 planned gravity orbits. We propagated the trajectory of the spacecraft over 48-hour arcs centered at the pericenter, starting from the latest reference trajectory available on the NASA/NAIF (Navigation and Ancillary Information Facility) server (https://naif.jpl.nasa.gov/pub/naif/JUNO/kernels/spk/). The microwave signal is affected by several noise sources during the two-way round-trip path to and from the spacecraft (Asmar et al, 2005). Propagation noises, caused by variations in the refractive index as the signal travels through Earth's troposphere and ionosphere and interplanetary plasma are the dominant disturbances for Juno. These noises are largely reduced using measurements from the Advanced Media Calibration System and multi-frequency link techniques (Bar-Sever et al, 2007; Mariotti and Tortora, 2013). According to Juno's noise model and to the results obtained from the analysis of the first two gravity passes (Iess et al, 2018), we added random Gaussian white noise on the simulated observables with a standard deviation of 1.4 mHz at Ka-band (corresponding to 12.9 μm/s) and 0.6 mHz at X-band (22.5 μm/s) at 60-s integration time.

The Doppler data from each observation arc are collected into a multi-arc least-square batch filter for the estimation process; that is, each gravity pass is treated independently and the data from each arc contribute both to the information matrix of the parameters common to the entire dataset (global parameters, for example the gravity field and tidal response of Jupiter), and to the information matrix of the parameters pertaining to that specific arc (local parameters, for example the position and velocity of Juno) (Milani et al, 2010). The multi-arc approach is necessary because the large gap between adjacent pericenter passes would result in unacceptably large propagated errors over the 52.9-day orbit.

3.3 Spacecraft dynamical model

The dynamical model used for both the simulation of the measurements and the parameter estimation accounts for the gravitational and relativistic perturbations from the solar system planets and the Sun. We adopted the planetary and satellite ephemerides from JPL's DE430 and JUP310 solutions (Folkner et al, 2014; Jacobson et al, 2013). The dynamical model includes Jupiter's gravity field up to degree 30 and order 4, as well as the satellite-dependent tidal perturbation from the Galilean satellites up to degree and order 4. The maximum degree of the harmonic coefficients considered in this analysis follows from the result of numerical simulations in Finocchiaro, 2013, in that it is the minimum set of parameters necessary to fit the data without overparameterizing the problem and thus overestimating the final formal uncertainty on the solve-for parameters. The maximum order of the tesseral gravity field, instead, is coherent with the degree-4 tidal perturbation included in the model, and accounts for possible effects that could be observable at the end of the mission associated with the presence of Jupiter's meridional wind flows and of normal modes (see Section 4). The nominal values of the gravity field coefficients follow latest estimates (Iess, et al, 2018) and are the same for both the data simulation and the parameter estimation processes. The motion of Jupiter's spin-axis is described by the IAU 2009 model (Archinal et al, 2011). The dynamical model includes also the planetary and albedo radiation, as well as the solar radiation pressure (see Finocchiaro, 2013 for details) and the Lense-Thirring acceleration, a relativistic frame-dragging effect caused by the rotation of Jupiter (Iorio, 2010), whose effect is proportional to Jupiter's angular momentum (the polar moment of inertia has been set to C = 0.26, in agreement with interior model predictions).

3.3.1 Satellite-dependent tidal model

The dynamical model used for the reference solution based on Juno's first two gravity-dedicated pericenter passages (Iess et al, 2018) includes only one Love number for each degree and order of the spherical harmonic expansion, which comprehends the total contribution from all the satellites (see Equation (2) and Moyer, 2003). In order to determine Juno's sensitivity to Jupiter's satellite-

dependent tides, we modified that model by defining one Love number k_{lm}^{j} for each satellite j (see Equation (4)) and computing the partial derivatives of the observable with respect to the new parameters independently during the estimation process.

$$\Delta\bar{J}_l = -\frac{1}{2l+1}\sum_j k_{l0}^{j}\frac{\mu_j}{\mu}\left(\frac{R}{r_j}\right)^{l+1}\bar{P}_{l0}(u_j), \tag{4}$$

$$\Delta\bar{C}_{lm} - i\Delta\bar{S}_{lm} = \frac{1}{2l+1}\sum_j k_{lm}^{j}\frac{\mu_j}{\mu}\left(\frac{R}{r_j}\right)^{l+1}\bar{P}_{lm}(u_j)(s_j - it_j)^m.$$

We only considered tides raised by Io, Europa and Ganymede and Callisto. The tidal perturbations due to Amalthea, Adrastea, Metis, Thebe and the Sun have not been included in this analysis since the tidal parameters of those bodies are all much lower than Callisto's (see Table 1), and numerical simulations carried out with the modified tidal model showed that the resulting gravitational signature on the Juno data would be well below the noise level.

We assumed the static Love numbers from Table 4 in Wahl et al, 2016 as nominal values for the k_{lm}^{j}, assuming Callisto's k_{lm} equal to the one of Ganymede. Note that the aim of our analysis is to report on the uncertainties on the satellite-dependent Love numbers, which do not depend on the actual values used in the simulation but only on the orbital geometry and the quality of the data.

3.4 Definition of the solve-for parameters

We set up the estimation filter with the following global solve-for parameters: Jupiter's gravitational parameter (μ), its gravity field coefficients up to degree 30 and order 4, Jupiter's pole position (Right Ascension (RA) and Declination (Dec)) and pole-rate, and its angular momentum (responsible for the Lense-Thirring effect). Moreover, we solved for k_{22}, k_{31}, k_{33}, k_{42}, k_{44} for Io, Europa, Ganymede and Callisto, as well as the masses of the Galilean satellites and Amalthea with apriori uncertainties according to the published JUP310 solution (Jacobson, 2013). The local solve-

for parameters are the position and velocity of the spacecraft at the beginning of each arc, with apriori uncertainties of 10 km and 10 mm/s, respectively. Both the gravity field coefficients and the Love numbers are unconstrained parameters.

Note that our simulations refer to the case where a static degree-4 tesseral field is required to fit the Doppler data. A static tesseral field, possibly due to meridional surface flows, may be required at end-of-mission, according to the penetration depth (Parisi et al, 2016; Galanti et al, 2017). The minimum degree needed to fit Juno gravity data will depend on the strength of such wind-induced tesseral gravity field, currently unknown. In addition, a time-variable tesseral field might arise as well, due to differential rotation inside Jupiter or to Jupiter's oscillations (Durante et al, 2017). With future gravity passes, the fine structure of Jupiter's gravity may be unveiled, and according to the strength of a possible tesseral field, the inclusion of additional parameters in the estimation process could degrade the uncertainties on the satellite-dependent Love numbers.

4. Results and discussion

In the following paragraphs, we present and discuss the results of the covariance analysis for the estimation of satellite-dependent Love numbers. Table 2 lists the 3-σ formal uncertainty on the Love numbers for Io, Europa, Ganymede and Callisto at the end of Juno's mission, suggesting good sensitivity to tides raised by the inner three satellites. In particular, the k_{22} of Io and Europa are determined (at 3-σ), respectively, to 0.84% and 13.1% of the static values (0.58999 and 0.58964 from Wahl et al, 2016, see also Figure 4).

Table 2: 3-σ formal uncertainty on Jupiter's satellite-dependent Love numbers at the end of the Juno mission.

	k_{22}	k_{31}	k_{33}	k_{42}	k_{44}

Io	0.005	0.015	0.014	0.086	0.071
Europa	0.081	0.209	0.319	3.957	2.340
Ganymede	0.094	0.191	0.659	10.69	7.470
Callisto	0.227	5.540	4.434	93.75	160.9

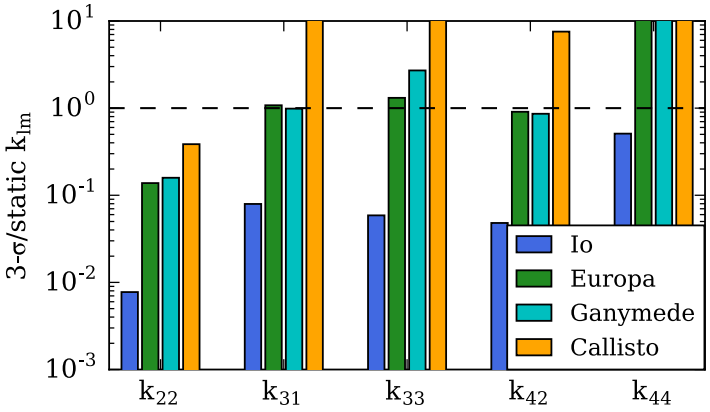

Figure 4: 3-σ formal uncertainty over static values from Wahl et al, 2016 for the Love numbers up to degree and order 4 for Io (blue), Europa (green), Ganymede (cyan) and Callisto (yellow). The horizontal dashed line corresponds to a ratio of one. Note that some of the values for Callisto are larger than 10.

As expected, the uncertainties on k_{lm} for the same degree and order scale approximately with the satellite tidal parameter q_T. Furthermore, since the tidal perturbation is proportional to $\left(R/r_j\right)^{l+1}$, the estimation uncertainty increases with l as well. The poor sensitivity to tides raised by Callisto is a consequence of the large semimajor axis of the satellite. The 1-σ uncertainty obtained on Io's k_{22} with the satellite-dependent tide model ($\sigma_{k_{22}^{Io}} = 1.71 \times 10^{-3}$, see Table 2) is about a factor-of-three larger than the uncertainty obtained on the same parameter with the frequency-independent tidal

model ($\sigma_{k_{22}} = 6.5 \times 10^{-4}$). This is caused both by the larger number of global parameters in the estimation filter, and by the large correlation between Io's and Europa's Love numbers (see below). Also, when estimating only one k_{lm} per degree and order of the perturbation, all the satellites provide information on that parameter, resulting in a better accuracy.

The dataset from the first two gravity-dedicated Juno perijoves (PJ03 and PJ06, see Iess et al, 2018), processed with the new satellite-dependent tidal model, provides an estimate for the tide raised by Io equal to ${k_{22}}^{Io} = 0.607 \pm 0.29$ (the uncertainty reported is equal to three times the formal uncertainty). The large uncertainty further confirms the need of data from the entire mission; however, the central value suggests that a certain degree of dynamical amplification of the Love numbers might be determined with Juno.

While the uncertainties in Table 2 reveal that the Juno gravity experiment is sensitive to the gravitational effect of satellite-dependent tides on Jupiter, the possibility of a separation of the contributions from each satellite can be assessed only by comparing the formal uncertainties with the actual values of the satellite-dependent Love numbers. For a preliminary assessment, we assumed a completely static response and used the Love numbers from the satellite-dependent model in Wahl et al, 2016 as central values (Figure 5). With this static model, the differences among the Love numbers of the satellites are quite small (dynamical effects can modify the Love numbers and thus amplify the differences among the satellites). The only exception is the Love number k_{42}, which shows the most notable variation among the Galilean satellites; however, the large uncertainties obtained on this parameter prevent a separation of the single tidal contributions.

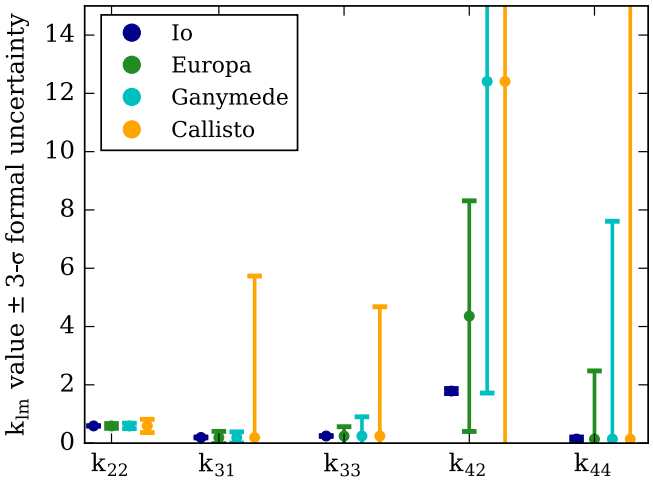

Figure 5: Satellite-dependent static Love numbers (dots) with the 3-σ formal uncertainties (vertical bars) retrieved from the covariance analysis. Some of the uncertainties (especially for Io) are so small that they cannot be correctly visualized in the plot. Please refer to Table 2 for the numerical values. Blue, green, cyan and yellow dots represent Io, Europa, Ganymede and Callisto, respectively.

As already introduced above, the uncertainties on the Love numbers are affected by a large correlation due to Juno's orbital period, which is almost resonant with that of the moon Io (see Section 2). The correlation matrix[1] associated with the satellite-dependent Love numbers (Figure 6) shows that this effect is most noticeable on Io's, Europa's and Ganymede's k_{22}, k_{31} and k_{42}.

[1] The correlation coefficient of two parameters 1-2 is defined as $\rho_{12} = \sigma_{12}/(\sigma_{11}\sigma_{22})$, where σ_{12} is the covariance of the 1-2 parameters (off-diagonal component in the variance-covariance matrix) and σ_{11}, σ_{22} are their standard deviations. The correlation matrix contains the correlation coefficients as off-diagonal elements.

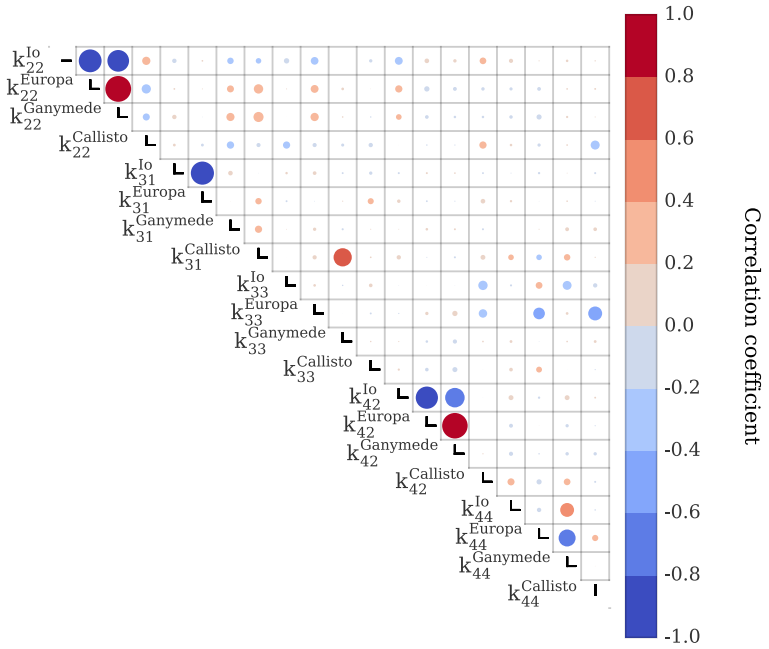

Figure 6: Correlation matrix for the Love numbers up to degree and order 4 for Io, Europa, Ganymede and Callisto. Green (purple) dots indicate a positive (negative) correlation coefficient. The correlation coefficient is also proportional to the size of the dots.

A small change of Juno's orbital period, such that the spacecraft does not encounter Io and Europa almost at the same longitudinal separation during each gravity pericenter, would strongly reduce the correlation. The new orbital period should still grant visibility from DSS 25 at pericenter and should not influence the scientific operation of the other instruments. We hypothesized that an impulsive maneuver could be performed on December 2019 to increase Juno's orbital period by 24 hours over the last 10 gravity orbits. The period change would be large enough to reduce the correlation, but it would not hinder the scientific goals of the mission.

We carried out the covariance analysis again with Juno's modified orbital period and computed the uncertainties on the satellite-dependent Love numbers. The results, shown in Figure 7, confirm that changing Juno's period would indeed decrease the correlations among the parameters. The effect

389 is most evident on k_{22} and k_{42}: the formal uncertainty of Io's k_{22} and k_{42} is about 75% of the values
390 with Juno's nominal period, while the uncertainty on Europa's and Ganymede's Love numbers
391 decreases by more than a factor of two. In particular, the 3-σ uncertainties on the k_{42} for Io, Europa
392 and Ganymede with the modified orbital period are, respectively, 0.07, 1.87 and 4.99. These values
393 would enable separating the single tidal contributions of the k_{42} due to Io, Europa and Ganymede in
394 the context of the static model by Wahl et al, 2016. However, dynamical tides can modify the central
395 values of the Love numbers. If this were the case, the contributions from the Galilean satellites might
396 be separated without the need to decrease the correlations by changing the orbital period of the
397 spacecraft (something that may be operationally challenging).
398

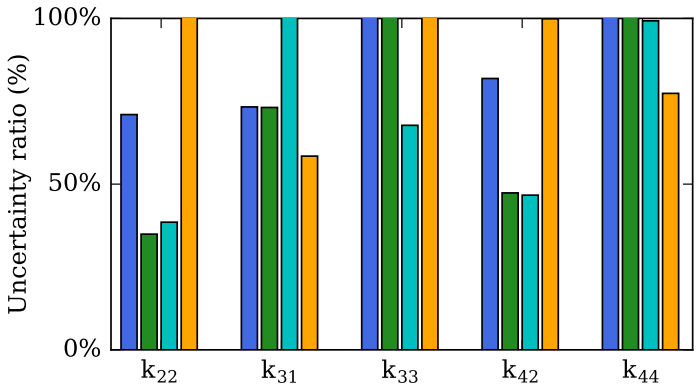

399

400 **Figure 7:** Uncertainties (percentage) on the satellite-dependent
401 static Love numbers for the modified Juno orbital period relative to
402 the ones for the nominal scenario. Blue, green, cyan and yellow bars
403 represent Io, Europa, Ganymede and Callisto, respectively.

404 We point out that the quoted uncertainties depend on the maximum degree and order of Jupiter's
405 tesseral gravity field expansion, currently set to 4. Numerical simulations show that the formal
406 uncertainties on the satellite-dependent Love numbers would increase by about 10% when including
407 a full degree-6 tesseral field. Of the contrary, if Jupiter's gravity is purely zonal (within the accuracy

of Juno's data), fewer parameters will be required to fit the data, therefore resulting in better accuracies for the Love numbers (about 20% lower when estimating only zonal harmonics).

5. Conclusions

We evaluated the sensitivity of the Juno gravity science experiment to satellite-dependent tides on Jupiter, raised by the Galilean satellites as they orbit around the planet with different orbital periods, each corresponding to a different forcing frequency. The gravitational signature of the tides can be observed by uniformly sampling the tidal bulges raised on Jupiter by its moons; consequently, Doppler measurements spanning the full duration of the Juno mission are required to obtain the best sensitivity.

We carried out realistic numerical simulations of the Juno gravity experiment and implemented the satellite-dependent tidal response of Jupiter in the dynamical model used to simulate and fit Juno Doppler data. The covariance analysis showed that Juno is indeed sensitive to satellite-dependent tides raised by Io, Europa and Ganymede. We did not include tides raised by other satellites or the Sun as their tidal parameters are much lower than Callisto's (see Table 1), and the corresponding acceleration on Juno would be negligible. We neglected the effect of the tidal perturbations of degree 5 and 6 for the same reason.

Currently, the only prediction of Jupiter's satellite-dependent Love numbers is provided by the static analysis in Wahl et al, 2016. If Jupiter's actual tidal response closely matched this prediction, our sensitivity analysis shows that it might not be possible to separate the tidal contributions coming from the different satellites with Juno gravity data with the nominal mission profile. Indeed, Juno's orbital period is nearly resonant with Io's, so that the sampling of the tidal bulge is nearly identical for Io, Europa and Ganymede (due to the Laplace resonance). The ensuing correlations increase the formal uncertainties of all Love numbers. We have shown that the separation of the tidal contributions from each satellite would be strongly facilitated if Juno's orbital period could be slightly changed

(e.g. by 24 hours). The break of the resonance would reduce the correlations and allow more than a two-fold improvement in the accuracy of k_{22} and k_{42}.

The possible detection of satellite-dependent tides on Jupiter would provide key information for further characterizing the interior structure of the planet. This paper has presented the predicted capabilities of the Juno gravity experiment. However, only further gravity data will allow to verify if the contributions of the different satellites can be successfully separated. As the spacecraft accumulates more pericenter passes, data from Juno processed with the satellite-dependent tidal model might reveal large discrepancies from a purely static response, providing insight into the interior of the planet through the analysis of the oscillation modes excited by the tidal perturbation (Fuller et al, 2016). The work presented in this paper, along with the results of the data analysis carried out as Juno progresses towards the end of the mission, would also contribute to the validation of dynamical tide models for gas giant planets. Finally, although in this work we considered only the real part of the Love numbers, a determination of the satellite-dependent imaginary part of the Love numbers, related to tidal dissipation inside the planet, would be valuable to determine the orbital evolution of the Jovian system.

Acknowledgements

The research described in this paper has been carried out at Sapienza University of Rome under an Italian Space Agency (ASI) sponsorship. MONTE is a NASA/JPL proprietary software used for deep-space navigation, while the multi-arc batch filter used for the covariance analysis has been developed at Sapienza University of Rome under contract with ASI. The authors want to thank the Juno Interior Working Group, in particular D. Stevenson, W. Hubbard and S. Wahl for suggesting the relevance of this topic.

References

Archinal, B.A., A'Hearn, M.F., Bowell, E., Conrad, A., Consolmagno, G.J., Courtin, R., Fukushima, T., Hestroffer, D., Hilton, J.L., Krasinsky, G.A., Neumann, G., Oberst, J., Seidelmann, P.K., Stooke, P., Tholen, D.J., Thomas, P.C., Williams I.P., *Report of the IAU working group on cartographic coordinates and rotational elements*, Celestial Mech. Dyn. Astron. 109:2 (2011), 101-135. https://doi.org/10.1007/s10569-010-9320-4

Asmar, S.W., Armstrong, J.W., Iess, L., Tortora, P., *Spacecraft Doppler tracking: noise budget and accuracy achievable in precision radio science observations*, Radio Sci. 40:2 (2005). https://doi.org/10.1029/2004RS003101

Asmar, S.W., Bolton, S.J., Buccino, D.R., Cornish, T.P., Folker, W.M., Fornaro, R., Iess, L., Jongeling, A.P., Lewis, D.K., Mittskus, A.P., Mukai, R., Simone, L., *The Juno gravity science instrument*, Space Sci. Rev. 213 (2017), 205-218. https://doi.org/10.1007/s11214-017-0428-7

Bar-Sever, Y.E., Jacobs, C.S., Keihm, S., Lanyi, G.E., Naudet, C.J., Rosenberger, H.W., Runge, T.F., Tanner, A.B., Vigue-Rodi, Y., *Atmospheric Media Calibration for the Deep Space Network*, Proc. of the IEEE 95:11 (2007), 2180-2192. https://doi.org/10.1109/JPROC.2007.905181

Bolton, S.J., Lunine, J., Stevenson, D., Connerney, J.E.P., Levin, S., Owen, T.C., Bagenal, F., Gautier, D., Ingersoll, A.P., Orton, G.S., Guillot, T., Hubbard, W., Bloxham, J., Coradini, A., Stephens, S.K., Mokashi, P., Thorne, R., Thorpe, R., *The Juno mission*, Space Sci. Rev. 213 (2017), 5-37. https://doi.org/10.1007/s11214-017-0429-6

Durante, D., Guillot, T., Iess, L., *The effect of Jupiter oscillations on Juno gravity measurements*, Icarus 282 (2017), 174-182. http://dx.doi.org/10.1016/j.icarus.2016.09.040

Finocchiaro, S., Numerical simulations of the Juno gravity experiment (PhD Thesis), Sapienza University of Rome, 2013.

Folkner, W.M., Williams, J.G., Boggs, D.H., Park, R.S., Kuchynka, P., *The Planetary and Lunar Ephemerides DE430 and DE431*, IPN Progress Report 42-196, 2014.

Fuller, J., Luan, J., Quataert, E., *Resonance locking as the source of rapid tidal migration in the Jupiter Saturn moon systems,* MNRAS 458:1 (2016), 3867-3879.

Galanti, E., Durante, D., Finocchiaro, S., Iess, L., Kaspi, Y., *Estimating Jupiter's Gravity Field Using Juno Measurements, Trajectory Estimation Analysis, and a Flow Model Optimization*, The Astronomical Journal 152:2 (2017), https://doi.org/10.3847/1538-3881/aa72db.

Gavrilov, S.V., Zharkov, V.N., Leontev, V.V., *Influence of tides on the gravitational field of Jupiter*, Soviet Astronomy 19:5 (1976), 618-621.

Gavrilov, S.V., Zharkov, V.N., *Love numbers of the giant planets*, Icarus 32:4 (1977), 443-449. https://doi.org/10.1016/0019-1035(77)90015-X

Guillot, T., Stevenson, D.J., Hubbard, W.B., Didier, S., The interior of Jupiter, *in:* Jupiter: the planet, satellites, and magnetosphere, *Cambridge University Press*, pp. 35-57 (2004).

Guillot, T., Miguel, Y., Militzer, B., Hubbard, W.B., Galanti, E., Kaspi, Y., Cao, H., Wahl, S., Iess, L., Folkner, W.M., Helled, R., Stevenson, D.J., Lunine, J.I., Reese, D., Biekman, A., Parisi, M.,

Durante, D., Connerney, J.E.P., Levin, S.M., Bolton, S. J., *A suppression of differential rotation in Jupiter's deep interior*, Nature 555 (2018), 227-230. https://doi.org/10.1038/nature25775

Iess, L., Folkner, W.M., Durante, D., Parisi, M., Kaspi, Y., Galanti, E., Guillot, T., Hubbard, W.B., Stevenson, D.J., Anderson, J.D., Buccino, D.R., Gomez Casajus, L., Milani, A., Park, R., Racioppa, P., Serra, D., Tortora, P., Zannoni, M., Cao, H., Helled, R., Lunine, J.I., Miguel, Y., Militzer, B., Wahl, S., Connerney, J.E.P., Levin, S.M., Bolton, S.J., *Measurement of Jupiter's asymmetric gravity field*, Nature 555 (2018), 220-222. https://doi.org/10.1038/nature25776

Iorio, L., *Juno, the angular momentum of Jupiter and the Lense-Thirring effect*, NewA 15 (2010), 554-560. https://doi.org/doi:10.1016/j.newast.2010.01.004

Jacobson, R. A., *JUP310 orbit solution* (2013), ftp://ssd.jpl.nasa.gov/pub/eph/satellites/nio/LINUX_PC/jup310xl.txt.

Kaspi, Y., Galanti, E., Hubbard, W.B., Stevenson, D.J., Bolton, S.J., Iess, L., Guillot, T., Bloxham, J., Connerney, J.E.P., Cao, H., Durante, D., Folkner, W.M., Helled, R., Ingersoll, A.P., Levin, S.M., Lunine, J.I., Miguel, Y., Militzer, B., Parisi, M., Wahl, S.M., *Jupiter's atmospheric jet streams extend thousands of kilometres deep*, Nature 555 (2018), 223-226. https://doi.org/10.1038/nature25793

Kaula, W., Theory of satellite geodesy, *Blaisdell ed*., 1966.

Lainey, V., Jacobson, R.A., Tajeddine, R., Cooper, N.J., Murray, C., Robert, V., Tobie, G., Guillot, T., Mathis, S., Remus, F., Desmars, J., Arlot, J-E., De Cuyper, J-P., Dehant, V., Pascu, D., Thuillot, W., Le Poncin-Lafitte, C., Zahn, J-P., *New constrains on Saturn's interior from Cassini astrometric data*, Icarus 281 (2017), 286-296. https://doi.org/10.1016/j.icarus.2016.07.014

Le Maistre, S., Folkner, W. M., Jacobson, R. A., Serra, D., *Jupiter spin-pole precession rate and moment of inertia from Juno radio-science observations*, Planetary Space Sci. 126 (2016), 78-92. https://doi.org/10.1016/j.pss.2016.03.006

Love, A.E.H., Some Problems of Geodynamics, *Cambridge University Press*, 1911.

Mariotti, G. and Tortora, P., *Experimental validation of a dual uplink multifrequency dispersive noise calibration scheme for Deep Space tracking*, Radio Sci. 48 (2013), 111-117. https://doi.org/10.1002/rds.20024

Milani, A. and Gronchi, G., Theory of Orbit Determination, *Cambridge University Press*, 2010.

Moyer, T. D., Formulation for observed and computed values of Deep Space Network data types for navigation, *John Wiley & Sons*, 2003.

Murray, C. D. and Dermott, S. F., Solar System Dynamics, *Cambridge University Press*, 1999.

Parisi, M., Galanti, E., Finocchiaro, S., Iess, L., Kaspi, Y., *Probing the depth of Jupiter's Great Red Spot with the Juno gravity experiment*, Icarus 267 (2016), 232-242. http://dx.doi.org/10.1016/j.icarus.2015.12.011

Smith, J., Taber, W., Drain, T., Evans, S., Evans, J., Guevara, M., Schulze, W., Sunseri, R., Wu, H-C., *MONTE Python for Deep Space Navigation*, Proc. of the 15th Python in Science Conf. (SCIPY 2016).

Vorontsov, S.V., Gavrilov, S.V., Zharkov, V.N., Leontev V.V., *Dynamical theory of the tides on the giant planets*, Astronomicheskii Vestnik 18 (1984), 8-18.

Wahl, S.M., Hubbard, W.B., Militzer, B., *Tidal response of a preliminary Jupiter model*, ApJ 831:14 (2016). https://doi.org/10.3847/0004-637X/831/1/14

Wahl, S.M., Hubbard, W.B., Militzer, B., *The Concentric MacLaurin Spheroid method with tides and a rotational enhancement of Saturn's tidal response*, Icarus 282 (2017), 183-194. https://doi.org/10.1016/j.icarus.2016.09.011

Wahl, S.M., Hubbard, W.B., Militzer, B., Guillot, T., Miguel, Y., Movshovitz, N., Kaspi, Y., Helled, R., Reese, D., Galanti, E., Levin, S., Connerney, J.E., Bolton, S.J., *Comparing Jupiter interior structure models to Juno gravity measurements and the role of a dilute core*, Geophys. Res. Lett. 44:10 (2017), 4649-4659. https://doi.org/10.1002/2017GL073160